

1
2
3
4
5
6
7
8
9
10
11
12
13
14
15
16
17
18
19
20
21
22
23

Phylogenomics places orphan protistan lineages in a novel eukaryotic super-group.

Matthew W. Brown^{1,2}, Aaron Heiss^{3,4}, Ryoma Kamikawa⁵, Yuji Inagaki^{6,7}, Akinori Yabuki⁸,
Alexander K Tice^{1,2}, Takashi Shiratori⁶, Ken-ichiro Ishida⁶, Tetsuo Hashimoto^{6,7}, Alastair G. B.
Simpson^{3*}, and Andrew J. Roger^{*}

1. Department of Biological Sciences, Mississippi State University USA
2. Institute for Genomics, Biocomputing & Biotechnology, Mississippi State University, USA
3. Centre for Comparative Genomics and Evolutionary Bioinformatics, Department of Biology
Dalhousie University, Halifax, N.S., B3H 4R2, Canada.
4. Department of Invertebrate Zoology and Sackler Institute for Comparative Genomics,
American Museum of Natural History, Central Park West at 79th St., New York, NY, 10024,
USA
5. Graduate School of Human and Environmental Studies, Graduate School of Global
Environmental Studies, Kyoto University, Japan
6. Graduate School of Life and Environmental Sciences, University of Tsukuba, 1-1-1
Tennodai, Tsukuba, Ibaraki 305-8572, Japan
7. Center for Computational Sciences, University of Tsukuba, 1-1-1 Tennodai, Tsukuba, Ibaraki
305-8577, Japan
8. Japan Agency for Marine-Earth Science and Technology (JAMSTEC), 2-15, Natsushima-cho,
Yokosuka, Kanagawa 237-0061, Japan.

24 9. Centre for Comparative Genomics and Evolutionary Bioinformatics, Dept. of Biochemistry
25 and Molecular Biology, Dalhousie University, Halifax, N.S., B3H 4R2, Canada

26 * **Corresponding Authors:** E-mail: Andrew.Roger@dal.ca and Alastair.Simpson@dal.ca

27

28

29 **Abstract**

30 Recent phylogenetic analyses position certain ‘orphan’ protist lineages deep in the tree of
31 eukaryotic life, but their exact placements are poorly resolved. We conducted phylogenomic
32 analyses that incorporate deeply sequenced transcriptomes from representatives of
33 collodictyonids (diphylleids), rigifilids, *Mantamonas* and ancyromonads (planomonads).
34 Analyses of 351 genes, using site-heterogeneous mixture models, strongly support a novel
35 supergroup-level clade that includes collodictyonids, rigifilids and *Mantamonas*, which we name
36 ‘CRuMs’. Further, they robustly place CRuMs as the closest branch to Amorphea (including
37 animals and fungi). Ancyromonads are strongly inferred to be more distantly related to
38 Amorphea than are CRuMs. They emerge either as sister to malawimonads, or as a separate
39 deeper branch. CRuMs and ancyromonads represent two distinct major groups that branch
40 deeply on the lineage that includes animals, near the most commonly inferred root of the
41 eukaryote tree. This makes both groups crucial in examinations of the deepest-level history of
42 extant eukaryotes.

43

44 **Introduction**

45 Our understanding of the eukaryote tree of life has been revolutionized by genomic and
46 transcriptomic investigations of diverse protists, which constitute the overwhelming majority of

47 eukaryotic diversity (Burki 2014; Simpson and Eglit 2016). Phylogenetic analyses of super-
48 matrices of proteins typically show a eukaryote tree consisting of five-to-eight ‘super-groups’
49 that fall within three even-higher-order assemblages: i) Amorphea (Amoebozoa plus Obazoa, the
50 latter including animals and fungi), ii) Diaphoretickes (primarily Sar, Archaeplastida, Cryptista
51 and Haptophyta), and iii) Excavata (Discoba and Metamonada) (Adl et al. 2012). Recent
52 analyses (Derelle et al. 2015) place the root of the eukaryote tree somewhere between Amorphea
53 and the other two listed lineages; Derelle *et al.* (2015) termed this the ‘Opimoda-Diphoda’ root.
54 There is considerable debate over the position of the root, however (e.g., (Cavalier-Smith 2010;
55 Katz et al. 2012; He et al. 2014))

56 Nonetheless, there remain several ‘orphan’ protist lineages that cannot be assigned to any
57 super-group by cellular anatomy or ribosomal RNA phylogenies (e.g., (Brugerolle et al. 2002;
58 Glücksman et al. 2011; Heiss et al. 2011; Cavalier-Smith 2013; Yabuki, Eikrem, et al. 2013;
59 Yabuki, Ishida, et al. 2013)). Recent phylogenomic analyses including *Collodictyon*,
60 *Mantamonas*, and ancyromonads indicate that these particular ‘orphans’ branch near the base of
61 Amorphea (Zhao et al. 2012; Cavalier-Smith et al. 2014), the same general position as the
62 purported Opimoda-Diphoda root. This implies, i) that these lineages are of special evolutionary
63 importance, but also, ii) that uncertainty over their phylogenetic positions will profoundly impact
64 our understanding of deep eukaryote history. Unfortunately their phylogenetic positions indeed
65 remain unclear, with different phylogenomic analyses supporting incompatible topologies, and
66 often showing low statistical support (Cavalier-Smith et al. 2014). This is likely due in part to the
67 modest numbers of sampled genes for some/most species examined to date (Cavalier-Smith et al.
68 2014; Torruella et al. 2015). Therefore, we undertook phylogenomic analyses that incorporated

69 deeply-sequenced transcriptome data from representatives of Collodictyonidae, *Mantamonas*,
70 Ancyromonadida, and Rigifilida.

71

72 **Results**

73 Using a custom phylogenomic pipeline plus manual curation we generated a dataset of 351
74 orthologs. The dataset was filtered of paralogs and potential cross-contamination by visualizing
75 each protein's phylogeny individually, then removing sequences whose positions conflicted with
76 a conservative consensus phylogeny (as in (Tice et al. 2016; Kang et al. 2017)) (supplementary
77 methods). We selected data-rich species to represent the phylogenetic diversity of eukaryotes.
78 Our primary dataset retained 61 taxa, with metamonads represented by two short-branching taxa
79 (*Trimastix* and *Paratrimastix*). We also analyzed a 64-taxon dataset containing three additional
80 longer-branching metamonads. Maximum likelihood (ML) and Bayesian analyses were
81 conducted using site-heterogeneous models; LG+C60+F+ Γ and the associated PMSF model
82 (LG+C60+F+ Γ -PMSF) as implemented in IQ-TREE (Wang et al. 2017) and CAT-GTR+ Γ in
83 PHYLOBAYES-MPI, respectively. Such site-heterogeneous models are important for deep-level
84 phylogenetic inference with numerous substitutions along branches (Lartillot et al. 2007; Le et
85 al. 2008; Wang et al. 2008; Pisani et al. 2015; Wang et al. 2017).

86 Our analyses of both 61- and 64-taxon datasets robustly recover well-accepted major
87 groups including Sar, Discoba, Metamonada, Obazoa, and Amoebozoa (Fig. 1, S1). Cryptista
88 (e.g. cryptomonads and close relatives) branches with Haptophyta (Fig. 1) in the LG+C60+F+ Γ -
89 PSMF analyses as well as in one set of two converged PHYLOBAYES-MPI chains under the CAT-
90 GTR model (Fig. S2). However another pair of converged chains places Haptophyta as sister to
91 Sar while Cryptista nests within Archaeplastida (Fig. S3), which is largely consistent with some

92 other recent phylogenomic studies (e.g., (Burki et al. 2016)). Excavata was never monophyletic,
 93 with Discoba forming a clan with Diaphoretickes taxa (Sar, Haptophyta,
 94 Archaeplastida+Cryptista) and Metamonada grouping with Amorphea plus the four orphan
 95 lineages targeted in this study (see below). Malawimonads, which are morphologically similar to
 96 certain metamonads and discobids (Simpson 2003), also branch amongst the ‘orphans’ (see
 97 below).



Figure 1. Phylogenetic tree for 61 eukaryotes, inferred from 351 proteins using Maximum Likelihood (LG+C60+F+Γ-PMSF model). The numbers on branches show (in order) support values from 100 real bootstrap replicates (LG+C60+F+Γ-PMSF model) and posterior probabilities both sets of converged chains in PHYLOBAYES-MPI under CAT-GTR+Γ model (i.e., MLBS/PP/PP). Filled circles represent maximum support with all methods; asterisks indicate a clade not recovered in the PHYLOBAYES analysis. Further, the dashed arrow indicates the placement of malawimonads inferred with PHYLOBAYES-MPI (see also inset summary tree), and grey arrows indicate the placements of other lineages in the PHYLOBAYES-MPI analyses.

99 Phylogenies of both datasets place all four orphan taxa near the base of Amorphea (Fig.
100 1, Fig. S1). The uncertain position of the eukaryotic root (discussed above) therefore makes it
101 unclear which bipartitions are truly clades, and which could be interrupted by the root. To allow
102 efficient communication, we discuss the phylogenies as if the orphan taxa all lie on the
103 Amorphea side of the root. We will also consider Amorphea as previously circumscribed (Adl et
104 al. 2012): the least-inclusive clade or clan containing Amoebozoa and Obazoa.

105 Three of the orphan lineages are specifically related in our trees (Fig. 1, S1). In both 61-
106 taxon and 64-taxon analyses, *Rigifila ramosa* (representing Rigifilida) forms a maximally-
107 supported clade with the collodictyonids *Collodictyon triciliatum* and *Diphylleia rotans*.
108 *Mantamonas plastica* then branches as their closest relative, with maximal support. This
109 Collodictyonid+Rigifilida+*Mantamonas* clade ('CRuMs') forms the sister group to Amorphea,
110 again with maximal support.

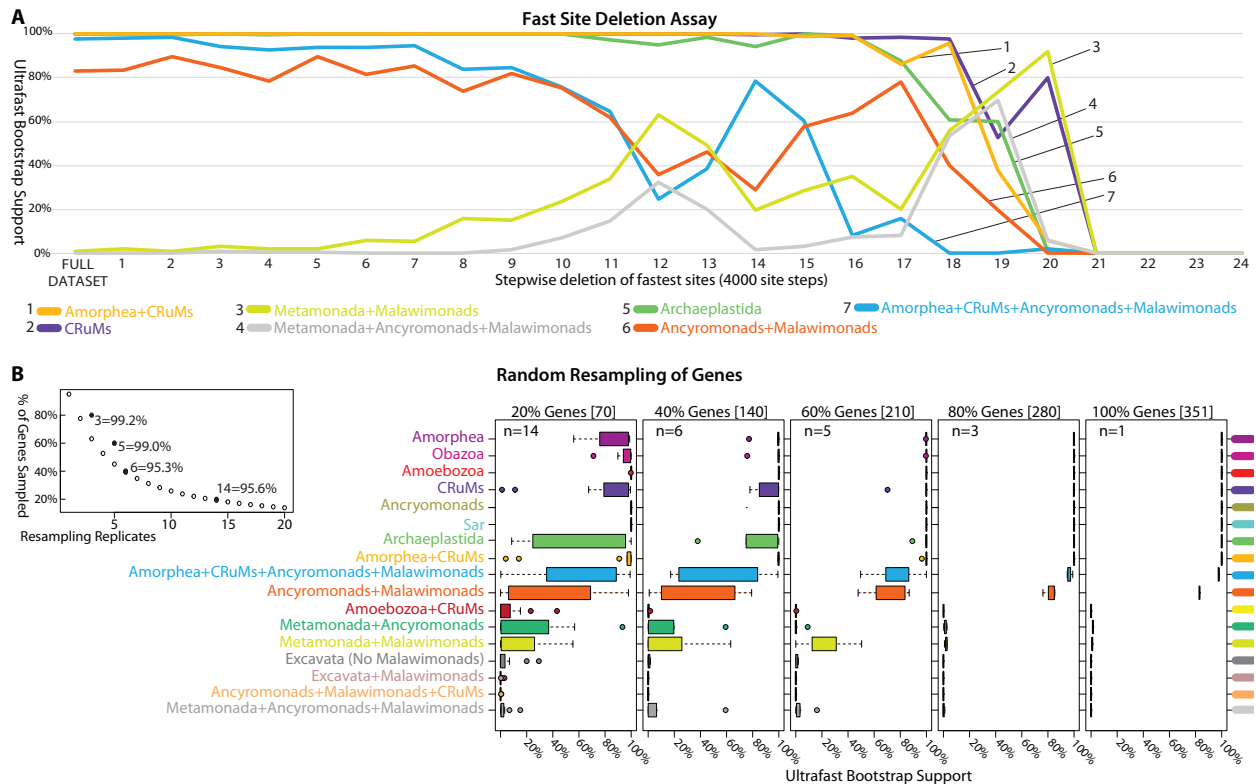
111 ML analyses and the converged PHYLOBAYES chains grouped ancyromonads,
112 malawimonads, and CRuMs with Amorphea, with strong bootstrap support and Bayesian
113 posterior probability (Fig. 1, 61 taxa; PMSF BS=98%, PP=1). Ancyromonads and
114 malawimonads formed a clade in the ML analyses, but with equivocal support (Fig. 1, 61 taxa;
115 BS=77%). Both sets of converged chains of the Bayesian analyses instead grouped
116 malawimonads with CRuMs+Amorphea to the exclusion of ancyromonads (Fig. S2, S3, PP=1
117 for both); however some unconverged chains support an ancyromonad+malawimonad clade
118 (data not shown). Lack of convergence amongst multiple chains using the CAT-GTR+ Γ model is
119 unfortunately common for large datasets, and often cannot be resolved by increasing the number
120 of generations of Markov chain Monte Carlo within a reasonable time frame (Pisani et al. 2015;

121 Kang et al. 2017). Instead we treat the two topologies recovered in these analyses as candidate
122 hypotheses requiring further investigation.

123

124 We conducted approximately unbiased (AU) topology tests on the 61-taxon data set
125 under the LG+C60+F+ Γ mixture model (Table S1). These tests rejected the Phylobayes trees, as
126 well as all trees optimized by enforcing constraints representing plausible alternative relative
127 placements of ancyromonads, malawimonads, and metamonads.

128 The fastest evolving sites are expected to be the most prone to saturation and systematic
129 error arising from model misspecification in phylogenomic analyses (Philippe et al. 2011). We
130 conducted a ‘fast-site removal’ analysis with the 61-taxon data set and generated ultrafast
131 bootstrap support (UFBOOT) values (Minh et al. 2013) for relevant groups as sites were
132 progressively removed from fastest to slowest (Fig. 2A). All groups of interest receive
133 reasonably strong support until ~44,000-48,000 sites were removed, when support fell markedly
134 for the ancyromonad+malawimonad clade and the
135 Amorphea+CRuMs+ancyromonad+*Malawimonas* clan. At this point, a notable proportion of the
136 bootstrap trees show malawimonads and/or ancyromonads grouping with metamonads. This
137 decline in support for the ancyromonad+malawimonad group reverses somewhat with further
138 site removal, before support falls again as overall phylogenetic structure is lost when ~76,000
139 sites are removed (Fig. 2A).



140

Figure 2. Effects of fast evolving sites and random subsampling of genes on our phylogenomic analyses. (A) Sites were sorted based on their rates of evolution estimated under the LG+F+ Γ model and removed from the data set from highest to lowest rate. Each step has 4,000 of the fastest evolving sites removed progressively. The bootstrap values (UFBOOT; LG+C60+F+ Γ -PSMF model) for each bipartition of interest are plotted. (B, C) Effects of random subsampling of genes within the 351-gene dataset. The following bipartitions were examined but received nearly 100% support across the fast site deletion assay (data not shown); Amorphea, Obazoa, Amoebozoa, Ancyromonads, and Sar. The following bipartitions were examined but received nearly 0% support across the fast site deletion assay (data not shown); Amoebozoa+CRuMs, Metamonada+Ancyromonads, Excavata (No Malawimonads), Excavata+Malawimonads, and Ancyromonads+Malawimonads+CRuMs. (B) Effects of random resampling of genes on the bipartitions of interest. Inset panel is the calculation of the number of replicates (n) necessary for a 95% probability of sampling every gene when subsampling 20, 40, 60 and 80% of genes using the formula: $0.95 = 1 - (1 - x/100)^n$ where x is the percentage of genes subsampled. UFBOOT support values for all nodes of interest with the variability of support values illustrated by box-and-whisker plots.

141

142 To evaluate heterogeneity in phylogenetic signals amongst genes (Inagaki et al. 2009),
143 we also inferred phylogenies from subsamples of the 351 examined genes (61-taxon dataset; Fig.
144 2B,C). For each subsample 20-80% of the genes were randomly selected, without replacement,
145 with replication as per Fig. 2B (giving a >95% probability that a particular gene would be
146 sampled at each level), and UFBOOT support for major clades was inferred (Fig. 2C). The ‘80%
147 retained’ replicates gave nearly identical results to the full dataset, indicating that there was little
148 stochastic error associated with gene sampling at this level. Support for the CRuMs clade is
149 almost always high when 40%+ of genes are retained, while subsamples containing 60% of
150 genes still showed differing support for a ancyromonad-malawimonad clade (as opposed to, for
151 example, malawimonads branching with metamonads).

152

153 **Discussion**

154 Our 351 protein (97,002 AA site) super-matrix places several orphan lineages in two separate
155 clades emerging between Amorphea and all other major eukaryote groups. All methods recover a
156 strongly supported clade comprising the free-swimming collodictyonid flagellates, the
157 idiosyncratic filose protist *Rigifila* (Rigifilida) and the gliding flagellate *Mantamonas*. This clade
158 is resilient to exclusion both of fast-evolving sites and of randomly selected genes. It is also
159 consistently placed as the immediate sister taxon to Amorphea. This represents the first robust
160 estimate of the positions of these three taxonomically poor but phylogenetically deep clades.
161 Previous phylogenomic analyses placed collodictyonids in various positions, such as sister to
162 either malawimonads or Amoebozoa, but often with low statistical support (Zhao et al. 2012;
163 Cavalier-Smith et al. 2014). Placements of *Mantamonas* have varied dramatically. A recent

164 phylogenomic study recovered a weak *Mantamonas*+collodictyonid clade in some analyses, but
165 other analyses in the same study instead recovered a weak *Mantamonas*+ancyromonad
166 relationship (Cavalier-Smith et al. 2014), and SSU+LSU rRNA gene phylogenies strongly
167 grouped *Mantamonas* with apusomonads (Glücksman et al. 2011; Yabuki, Ishida, et al. 2013).
168 Our study decisively supports the first of these possibilities. This is the first phylogenomic
169 analysis incorporating Rigifilida: Previous SSU+LSU rRNA gene analyses recovered a
170 negligibly supported collodictyonid+rigifilid clade, but not a relationship with *Mantamonas*
171 (Yabuki, Ishida, et al. 2013).

172 Overall, the hypotheses that i) collodictyonids, rigifilids and *Mantamonas* form a major
173 eukaryote clade, and ii) this clade is sister to Amorphea, are novel, plausible, and evolutionarily
174 important. No name exists for this putative super-group, and it is obviously premature to propose
175 a formal taxon. We suggest the place-holding moniker ‘CRuMs’ (Collodictyonidae, Rigifilida,
176 *Mantamonas*), which is euphonic and evokes the species-poor nature of these taxa.

177 Whether ancyromonads branch outside Amorphea or within it has been disputed (Paps et
178 al. 2013; Cavalier-Smith et al. 2014). Our study strongly places ancyromonads outside
179 Amorphea, more distantly related to it than are the CRuMs. Ancyromonads instead fall
180 ‘amongst’ the excavate lineages (Discoba, Metamonada, and Malawimonadidae). Resolving the
181 relationships amongst ‘excavates’ is extremely challenging (Hampl et al. 2009; Derelle et al.
182 2015), and this likely contributed to our difficulty in resolving the exact position of
183 ancyromonads vis-à-vis malawimonads. A close relationship between ancyromonads and
184 some/all excavates would be broadly consonant with the marked cytoskeletal similarity between
185 *Ancyromonas* and ‘typical excavates’ (Heiss et al. 2011). Certainly, our study flags
186 ancyromonads as highly relevant to resolving relationships amongst excavates.

187 Both candidate positions for ancyromonads place them at the centre of a crucial open
188 question: locating the root of the eukaryote tree. As discussed above, the latest analyses (Derelle
189 et al. 2015) locate the root between Discoba+Diaphoretickes ('Diphoda') and a clade including
190 Amorphea, colodictyonids and malawimonads ('Opimoda'). Our phylogenies show the
191 ancyromonad lineage emerging close to this split. One of the two positions we recovered would
192 actually place ancyromonads either as the deepest branch within 'Diphoda', or the deepest
193 branch within 'Opimoda', or even as sister to all other extant eukaryotes. This demonstrates the
194 profound importance of including ancyromonads in future rooted phylogenies of eukaryotes,
195 using datasets optimized for this purpose.

196

197 **Materials and Methods**

198 Details of experimental methods for culturing, nucleic acid extraction and Illumina sequencing
199 are described in the supplemental text.

200

201 *Phylogenomic data set construction.*

202 A reference data set of 351 aligned proteins described in (Kang et al. 2017) was used as the
203 starting point for the current analysis, from which 61 or 64 taxa representing diverse eukaryotes
204 were selected (see Table S2). Extensive efforts were made to exclude contamination and
205 paralogs, as described in the supplemental text. Poorly aligned sites were excluded using BMGE
206 (Criscuolo and Gribaldo 2010), resulting in an alignment of 97,002 amino acid (AA) sites with
207 less than 25% missing data for both 61- and 64-taxon datasets (Table S2).

208

209 *Phylogenomic tree inference*

210 Maximum likelihood (ML) trees were inferred using IQ-TREE v. 1.5.5 (Nguyen et al. 2015). The
211 best-fitting available model based on the Akaike Information Criterion (AIC) was the
212 LG+C60+F+ Γ mixture model with class weights optimized from the dataset and four discrete
213 gamma (Γ) categories. ML trees were estimated under this model for both 61- and 64-taxon data
214 sets. We then used this model and best ML tree under the LG+C60+F+ Γ model to estimate the
215 ‘posterior mean site frequencies’ (PMSF) model (Wang et al. 2017) for both 61 (Fig. 1) and 64
216 (Fig. S1) taxon data sets. This LG+C60+F+ Γ -PMSF model was used to re-estimate ML trees,
217 and for a bootstrap analysis of the 61-taxon dataset, with 100 pseudoreplicates (Fig. 1). AU
218 topology tests under the LG+C60+F+ Γ were conducted with IQ-TREE to evaluate whether trees
219 recovered by the Bayesian analyses or alternative placements of the orphan taxa could be
220 rejected statistically.

221 Bayesian inferences were performed using PHYLOBAYES-MPI v1.6j (Rodrigue and
222 Lartillot 2014), under the CAT-GTR+ Γ model, with four discrete Γ categories. For the 61-taxon
223 analysis, 6 independent Markov chain Monte Carlo chains were run for ~4,000 generations,
224 sampling every second generation. Two sets of two chains converged (at 800 and 2,000
225 generations, which were respectively used as the burnin), with the largest discrepancy in
226 posterior probabilities (PPs) (maxdiff) < 0.05. The topologies of the converged chains are
227 presented in Fig. S3 and S4 and are mapped upon Fig. 1. For the 64-taxon analysis, four chains
228 were run for ~3,000 generations. Two chains converged at ~200 generations, which was used as
229 the burnin, (maxdiff = 0) and the posterior probabilities are mapped upon the ML tree in Fig. S1.

230

231 *Fast-site removal and gene subsampling analyses*

232 For fast site removal, rates of evolution at each site of the 61-taxon dataset were estimated with
233 DIST_EST (Susko et al. 2003) under the LG model using discrete gamma probability estimation.
234 A custom PYTHON script was then used to remove fastest evolving sites in 4,000-site steps.
235 Random subsampling of 20, 40, 60, or 80% of the genes in the 61-taxon dataset was conducted
236 using a custom PYTHON script, with the number of replicates as given in Fig 2B. In both cases
237 each step or subsample was analyzed using 1,000 UFBOOT replicates in IQ-TREE under the
238 LG+C60+F+ Γ -PMSF model.

239

240 *Data availability*

241 All new transcriptomic data have been deposited at the National Center for Biotechnology
242 Information under BioProjects PRJNA401035, as detailed in Table S1. All single gene
243 alignments, masked and unmasked, and phylogenomic matrices are available in supplemental
244 file Brown_etal.2017.CRuMs.tgz

245

246 **Acknowledgements**

247 The authors thank Tom Cavalier-Smith and Ed Glücksman (Oxford University) for supplying
248 cultures strains B-70 (*Ancyromonas sigmoides*), NYK3C (*Fabomonas tropica*), and Bass1
249 (*Mantamonas plastica*). The part of this work conducted at Dalhousie University was supported
250 by NSERC Discovery grants awarded to AGBS (298366-2014) and AJR (2016-06792)
251 respectively. AJR also acknowledges the Canada Research Chairs program for support. This
252 project was supported in part by the National Science Foundation (NSF) Division of
253 Environmental Biology (DEB) grant 1456054 (<http://www.nsf.gov>), awarded to MWB.
254 Mississippi State University's High Performance Computing Collaboratory provided some

255 computational resources. The part of this work conducted at the University of Tsukuba was
256 supported by grants from the Japan Society for the Promotion of Science (JSPS; 15H05606 and
257 15K14591 awarded to RK, 23117006 and 16H04826 awarded to YI, 15H04411 awarded to KI,
258 and 15H05231 to TH) and by the "Tree of Life" research project (Univ. Tsukuba).

259 **References**

- 260 Adl SM, Simpson AGB, Lane CE, Lukeš J, Bass D, Bowser SS, Brown MW, Burki F, Dunthorn
261 M, Hampl V, et al. 2012. The revised classification of eukaryotes. *J. Eukaryot. Microbiol.*
262 59:429–493.
- 263 Brugerolle G, Bricheux G, Philippe H, Coffea G. 2002. *Collodictyon triciliatum* and *Diphylleia*
264 *rotans* (= *Aulacomonas submarina*) form a new family of flagellates (Collodictyonidae)
265 with tubular mitochondrial cristae that is phylogenetically distant from other flagellate
266 groups. *Protist* 153:59–70.
- 267 Burki F. 2014. The eukaryotic tree of life from a global phylogenomic perspective. *Cold Spring*
268 *Harb. Perspect. Biol.* 6:a016147.
- 269 Burki F, Kaplan M, Tikhonenkov DV, Zlatogursky V, Minh BQ, Radaykina LV, Smirnov A,
270 Mylnikov AP, Keeling PJ. 2016. Untangling the early diversification of eukaryotes: a
271 phylogenomic study of the evolutionary origins of Centrohelida, Haptophyta and
272 Cryptista. *Proc. Biol. Sci.* 283.
- 273 Cavalier-Smith T. 2010. Kingdoms Protozoa and Chromista and the eozoan root of the
274 eukaryotic tree. *Biol. Lett.* 6:342–345.
- 275 Cavalier-Smith T. 2013. Early evolution of eukaryote feeding modes, cell structural diversity,
276 and classification of the protozoan phyla Loukozoa, Sulcozoa, and Choanozoa. *Eur. J.*
277 *Protistol.* 49:115–178.
- 278 Cavalier-Smith T, Chao EE, Snell EA, Berney C, Fiore-Donno AM, Lewis R. 2014. Multigene
279 eukaryote phylogeny reveals the likely protozoan ancestors of opisthokonts (animals,
280 fungi, choanozoans) and Amoebozoa. *Mol. Phylogenet. Evol.* 81:71–85.
- 281 Criscuolo A, Gribaldo S. 2010. BMGE (Block Mapping and Gathering with Entropy): a new
282 software for selection of phylogenetic informative regions from multiple sequence
283 alignments. *BMC Evol. Biol.* 10:210.
- 284 Derelle R, Torruella G, Klimeš V, Brinkmann H, Kim E, Vlček Č, Lang BF, Eliáš M. 2015.
285 Bacterial proteins pinpoint a single eukaryotic root. *Proc. Natl. Acad. Sci. U. S. A.*
286 112:E693–699.

- 287 Glücksman E, Snell EA, Berney C, Chao EE, Bass D, Cavalier-Smith T. 2011. The novel marine
288 gliding zooflagellate genus *Mantamonas* (Mantamonadida ord. n.: Apusozoa). *Protist*
289 162:207–221.
- 290 Hampl V, Hug L, Leigh JW, Dacks JB, Lang BF, Simpson AGB, Roger AJ. 2009. Phylogenomic
291 analyses support the monophyly of Excavata and resolve relationships among eukaryotic
292 “supergroups.” *Proc. Natl. Acad. Sci. U. S. A.* 106:3859–3864.
- 293 He D, Fiz-Palacios O, Fu C-J, Fehling J, Tsai C-C, Baldauf SL. 2014. An alternative root for the
294 eukaryote tree of life. *Curr. Biol.* CB 24:465–470.
- 295 Heiss AA, Walker G, Simpson AGB. 2011. The ultrastructure of *Ancyromonas*, a eukaryote
296 without supergroup affinities. *Protist* 162:373–393.
- 297 Inagaki Y, Nakajima Y, Sato M, Sakaguchi M, Hashimoto T. 2009. Gene sampling can bias
298 multi-gene phylogenetic inferences: the relationship between red algae and green plants
299 as a case study. *Mol. Biol. Evol.* 26:1171–1178.
- 300 Kang S, Tice AK, Spiegel FW, Silberman JD, Pánek T, Cepicka I, Kostka M, Kosakyan A,
301 Alcântara DM, Roger AJ, et al. 2017. Between a pod and a hard test: the deep evolution
302 of amoebae. *Mol. Biol. Evol.*
- 303 Katz LA, Grant JR, Parfrey LW, Burleigh JG. 2012. Turning the crown upside down: gene tree
304 parsimony roots the eukaryotic tree of life. *Syst. Biol.* 61:653–660.
- 305 Lartillot N, Brinkmann H, Philippe H. 2007. Suppression of long-branch attraction artefacts in
306 the animal phylogeny using a site-heterogeneous model. *BMC Evol. Biol.* 7 Suppl 1:S4.
- 307 Le SQ, Lartillot N, Gascuel O. 2008. Phylogenetic mixture models for proteins. *Philos. Trans. R.*
308 *Soc. Lond. B. Biol. Sci.* 363:3965–3976.
- 309 Minh BQ, Nguyen MAT, von Haeseler A. 2013. Ultrafast approximation for phylogenetic
310 bootstrap. *Mol. Biol. Evol.* 30:1188–1195.
- 311 Nguyen L-T, Schmidt HA, von Haeseler A, Minh BQ. 2015. IQ-TREE: a fast and effective
312 stochastic algorithm for estimating maximum-likelihood phylogenies. *Mol. Biol. Evol.*
313 32:268–274.
- 314 Paps J, Medina-Chacón LA, Marshall W, Suga H, Ruiz-Trillo I. 2013. Molecular phylogeny of
315 unikonts: new insights into the position of apusomonads and ancyromonads and the
316 internal relationships of opisthokonts. *Protist* 164:2–12.
- 317 Philippe H, Brinkmann H, Lavrov DV, Littlewood DTJ, Manuel M, Wörheide G, Baurain D.
318 2011. Resolving difficult phylogenetic questions: why more sequences are not enough.
319 *PLoS Biol.* 9:e1000602.

- 320 Pisani D, Pett W, Dohrmann M, Feuda R, Rota-Stabelli O, Philippe H, Lartillot N, Wörheide G.
321 2015. Genomic data do not support comb jellies as the sister group to all other animals.
322 Proc. Natl. Acad. Sci. U. S. A. 112:15402–15407.
- 323 Rodrigue N, Lartillot N. 2014. Site-heterogeneous mutation-selection models within the
324 PhyloBayes-MPI package. Bioinformatics 30:1020–1021.
- 325 Simpson AGB. 2003. Cytoskeletal organization, phylogenetic affinities and systematics in the
326 contentious taxon Excavata (Eukaryota). Int. J. Syst. Evol. Microbiol. 53:1759–1777.
- 327 Simpson AGB, Eglit Y. 2016. Protist Diversification. In: Encyclopedia of Evolutionary Biology.
328 Vol. 3. Elsevier. p. 344–360.
- 329 Susko E, Field C, Blouin C, Roger AJ. 2003. Estimation of rates-across-sites distributions in
330 phylogenetic substitution models. Syst. Biol. 52:594–603.
- 331 Tice AK, Shadwick LL, Fiore-Donno AM, Geisen S, Kang S, Schuler GA, Spiegel FW,
332 Wilkinson KA, Bonkowski M, Dumack K, et al. 2016. Expansion of the molecular and
333 morphological diversity of Acanthamoebidae (Centramoebida, Amoebozoa) and
334 identification of a novel life cycle type within the group. Biol. Direct 11:69.
335
- 336 Torruella G, de Mendoza A, Grau-Bové X, Antó M, Chaplin MA, del Campo J, Eme L, Pérez-
337 Córdón G, Whipps CM, Nichols KM, et al. 2015. Phylogenomics Reveals Convergent
338 Evolution of Lifestyles in Close Relatives of Animals and Fungi. Curr. Biol. 25:2404–
339 2410.
- 340 Wang H, Minh B, Susko E, Roger AJ. 2017. Modeling Site Heterogeneity with Posterior Mean
341 Site Frequency Profiles Accelerates Accurate Phylogenomic Estimation. Syst. Biol. in
342 press.
- 343 Wang H-C, Li K, Susko E, Roger AJ. 2008. A class frequency mixture model that adjusts for
344 site-specific amino acid frequencies and improves inference of protein phylogeny. BMC
345 Evol. Biol. 8:331.
- 346 Yabuki A, Eikrem W, Takishita K, Patterson DJ. 2013. Fine structure of *Telonema subtilis*
347 Griessmann, 1913: a flagellate with a unique cytoskeletal structure among eukaryotes.
348 Protist 164:556–569.
- 349 Yabuki A, Ishida K-I, Cavalier-Smith T. 2013. *Rigifila ramosa* n. gen., n. sp., a filose apusozoan
350 with a distinctive pellicle, is related to *Micronuclearia*. Protist 164:75–88.
- 351 Zhao S, Burki F, Bråte J, Keeling PJ, Klaveness D, Shalchian-Tabrizi K. 2012. *Collodictyon*--an
352 ancient lineage in the tree of eukaryotes. Mol. Biol. Evol. 29:1557–1568.